PAPER • **OPEN ACCESS**

Segmenting spatter particles on additively manufactured surfaces using deep learning

To cite this article: Hwee Ping Ng *et al* 2025 *Surf. Topogr.: Metrol. Prop.* **13** 015006

Surface Topography: Metrology and Properties

PAPER

Segmenting spatter particles on additively manufactured surfaces using deep learning

Hwee Ping Ng[1], **Qijian Chan**[1], **Zheng Jie Tan**[1], **Ronnie Ssebaggala**[1,2] and **Joseph John Lifton**[1,3]

[1] Advanced Remanufacturing & Technology Centre (ARTC), Agency for Science, Technology and Research (A*STAR), 3 CleanTech Loop, #01-01 CleanTech Two, Singapore, 637143, Singapore
[2] EPSRC Future Advanced Metrology Hub, Centre for Precision Technologies, School of Computing and Engineering, University of Huddersfield, Huddersfield HD1 3DH, United Kingdom
[3] Mechanical Engineering, Faculty of Engineering and Physical Sciences, University of Southampton, Southampton, SO17 1BJ, United Kingdom

E-mail: J.J.Lifton@soton.ac.uk

Keywords: surface roughness, additive manufacturing, deep learning, U-net

OPEN ACCESS

RECEIVED
21 August 2024

REVISED
18 November 2024

ACCEPTED FOR PUBLICATION
7 January 2025

PUBLISHED
15 January 2025

Abstract

Metal additively manufactured (AM) surfaces do not exhibit the same surface features as machined surfaces. Rather than cutting marks, the additive surface may display surface features such as spatter particles, weld tracks, cracks, and surface breaking pores. These features are not well described by surface height parameters that were developed for machined surfaces. Therefore, an AM specific surface characterisation approach is required; feature based surface characterisation is a promising approach, but it requires surface features to be manually segmented which is a subjective process. In this work, a U-Net spatter particle segmentation algorithm is developed that removes the subjectivity of manual surface feature segmentation. A U-Net model is trained to segment spatter particles from optical measurements of 20 different metal AM samples. The performance of the U-Net segmentation algorithm is compared to segmenting the spatter particles using manual thresholding. The results show that the U-Net segmentation approach outperforms manual segmentations for 2 of 3 test samples considered. It is found that for 2 of 3 samples, the U-Net segmentation algorithm detects spatter particles that are missed by the manual segmentation approach. It is concluded that further training of the U-Net approach is required before it can fully supersede manual segmentation. In the future, it may be possible to replace human operators that subjectively segment surface features with robust machine learning-based surface feature segmentation algorithms. This novel application of U-Net for AM surface feature segmentation has the potential to automate surface characterisation for metal AM process optimisation, and for quality control in production environments.

1. Introduction

Additive manufacturing (AM) enables the fabrication of intricate metal components, however, the assessment of the surface quality of AM components remains challenging. When compared to machined surfaces, AM surfaces tend to have higher roughness and very different surface features, making traditional methods of surface roughness characterisation less meaningful. Therefore, there is a need for new approaches to characterise AM surface quality and relating it to the intended function of the surface. Traditional surface roughness characterisation methods assume a random surface height distribution, which does not align well with AM surfaces. It is apparent that a feature-based characterisation approach would be more logical and insightful, such an approach involves segmenting individual surface features and evaluating their dimensional and spatial attributes. Currently, segmenting surface features in AM components relies on human operators who select threshold values or employ subjective segmentation algorithms like watershed segmentation [1]. This subjectivity introduces variability in the surface characterisation and hampers the reliability of the assessment. Therefore, there is a need for a non-subjective feature segmentation approach. In our work, we explore the implementation of a convolutional neural

network based segmentation algorithm to achieve a less subjective approach to assessing the surface quality of AM components.

Feature-based surface characterisation is a well-established approach to surface texture metrology. It involves the isolation and dimensional evaluation of pertinent topographic formations. This method diverges from techniques that offer a broad statistical overview of the surface, instead providing a more comprehensive understanding of individual features. These features can encompass elements such as peaks, valleys, ridges, and furrows, contingent on the surface's nature. Each feature is quantified based on its geometric properties (e.g., area, width, height) and an entire surface can be characterised by the statistical properties of feature aggregations [2]. By concentrating on individual features, a more detailed comprehension of the surface texture can be achieved. Patterns and structures that might be overlooked by a basic statistical analysis can be detected. This is particularly beneficial in areas like additive manufacturing where minor variations in surface texture can significantly impact a part's performance, such as the presence of a partially fused particle, or a surface breaking crack.

Segmentation, an essential step in feature-based characterisation, involves dividing the measured surface topography into regions to separate the targeted features from their surroundings [3]. The precision of defining the geometric boundaries of each feature directly influences the calculation of the feature's geometric properties [4]. Previous work has investigated the use of morphologic segmentation algorithms for segmenting and characterising individual surface features [5], however, such an approach requires an expert user to select the segmentation parameters, which introduces subjectivity to the segmentation process. This subjectivity can be overcome by using a machine learning segmentation approach, where no human judgement is required to segment surface features.

Machine learning is increasingly used in additive manufacturing process control: from establishing correlations between process parameters and surface texture measurements [6], predicting a material's properties based on print parameters [7], isolating spattered material during the AM process [8], segmenting particles from shadowgraphs [9], segmenting particles from mineral samples acquired with micro-CT [10], classifying spatter using acoustic signals during the AM process [11], and predicting the porosity of AM parts [12]. In this study, we employ the U-Net deep learning architecture to segment and subsequently characterise spatter particles from areal surface topography data of AM samples. We choose to focus on the segmentation of spatter particles as they are a well-defined metal AM surface feature that have a direct impact on the overall surface quality and mechanical properties of a component [13].

U-Net, originally designed for biomedical image segmentation [14], offers a tailored architecture optimised for discerning intricate shapes and fine details in image segmentation tasks. The U-Net architecture has been applied for identifying layer-wise porosity defects in metal AM processes [15], however it has not yet been used for segmenting spatter particles for AM surface quality assessment. This novel application of U-Net for segmenting spatter particles is expected to overcome the subjectivity associated with manual surface feature segmentation, leading to improved surface quality assessment that can be used for quality assurance in production environments, or for AM process parameter optimisation.

2. Methods

The methodology adopted is as follows: a set of metal AM samples are fabricated with varying degrees of surface roughness (section 2.1); the AM surfaces are measured optically (section 2.2); a method for segmenting spatter particles manually is presented in section 2.3, and the U-Net segmentation model is described in section 2.4; results of the U-Net spatter particle segmentation method are presented in section 3 and compared to the manual segmentation approach.

2.1. Test samples

A total of 23 $10 \times 10 \times 10$ mm^3 test cubes are fabricated, an example test cube is shown in figure 1. The cubes are produced using an EOS M290 laser powder bed fusion system (EOS GmbH from Germany) and EOS AlSi10 Mg powder.

During the printing of the test cubes, five key print parameters are varied: infill laser power, infill scan speed, infill hatch distance, contour laser power, and contour scan speed. Here, we use the contour laser power and contour scan speed to influence the surface quality. Surface texture improves when laser power is increased towards an optimal value as the higher laser power gives rise to a wider melt pool [16–18], but deteriorates past the optimal laser power due to hump formation [17]. Higher scan speeds past an optimal value results in porosity, discontinuities and cracks, resulting in a rougher surface [16, 18]. The infill exposure parameter is also varied so that the cubes can be reused for further porosity studies, but this should not affect the surface quality. The full exposure parameters are presented for completeness in the table of print settings in the appendix.

Three out of the 23 fabricated cubes are designated for testing the trained U-Net model, note that the surfaces of the 3 test cubes are not used to train the U-Net model. The test surfaces exhibit distinct features from one another, enabling a comprehensive evaluation of the model's performance. The selected surfaces are from the cubes: I11, I9, and G1.

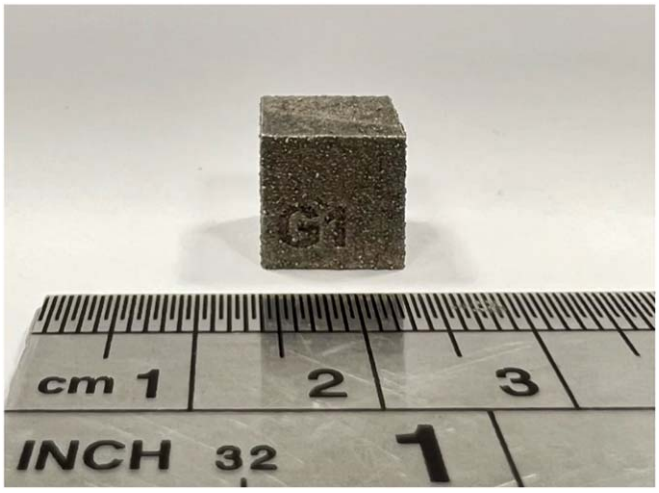

Figure 1. An example of the AM samples used to test the developed machine learning spatter particle segmentation method.

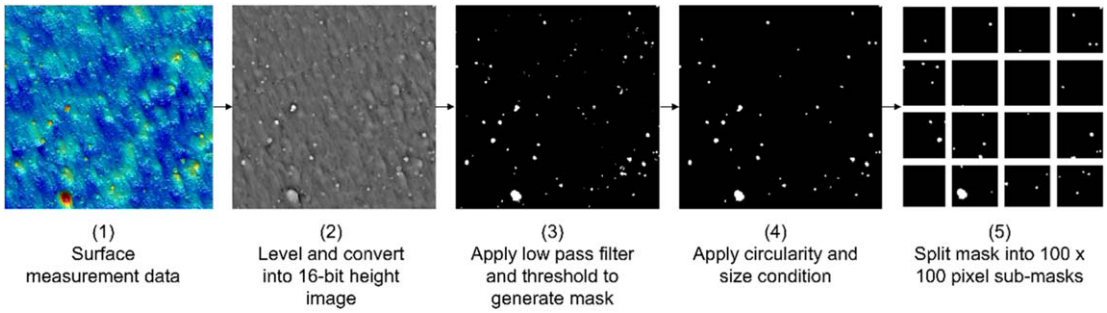

Figure 2. Pipeline for segmenting spatter particles on AM surfaces using manual thresholding.

2.2. Optical measurement of surfaces

The test cubes′ surfaces are measured using the Alicona Infinite Focus G4 optical focus variation microscope (Bruker Alicona Imaging GmbH, Austria). This high-precision system records the 3D surface height data which is then stored as a text file of x, y, z surface coordinates. These datasets are used to create surface images for manual spatter segmentation and the U-Net model training.

The optical measurement settings are as follows: 10 μm lateral resolution, 1 μm vertical resolution, 5× magnification utilising coaxial illumination. A measurement area of 7 mm by 7 mm is extracted per scanned surface for analysis.

2.3. Spatter particle segmentation using manual thresholding

Spatter particle segmentation employing manual thresholding encompasses a series of data processing steps. Initial preprocessing involves cropping the surface data into a square region of 6 mm by 6 mm. Following this, a leveling operation is executed by fitting a least squares plane and subtracting it from the surface. A high pass filter is then applied to remove form and waviness. Subsequently, the data undergoes a thresholding process based on the z height of the surface; this operation isolates predominant particle features, yielding a binary mask wherein pixel values indicate spatter particle presence or absence. In a subsequent stage of processing, blob detection is used to remove particles smaller than 3 × 3 pixels, it is assumed that the lateral sampling resolution of the surface measurement is insufficient to resolve such particles. Furthermore, particles with a circularity lower than 0.5 to 0.7 are removed, this is done based on the assumption that spatter particles are approximately circular in shape. The workflow for segmenting spatter particles using manual thresholding is shown in figure 2.

2.4. Spatter particle segmentation using U-Net

The U-Net model undergoes training using 20 of the manually segmented datasets. The measured surface data is converted into a 16-bit greyscale image and then split into 100 × 100-pixel sub images. The particle masks generated from the manual segmentation are also split into 100 × 100-pixel sub masks. Thus, the U-Net model is trained on the sub-images and corresponding sub-masks. Through the training process the U-Net model learns patterns and features in order to distinguish spatter particles in the surface

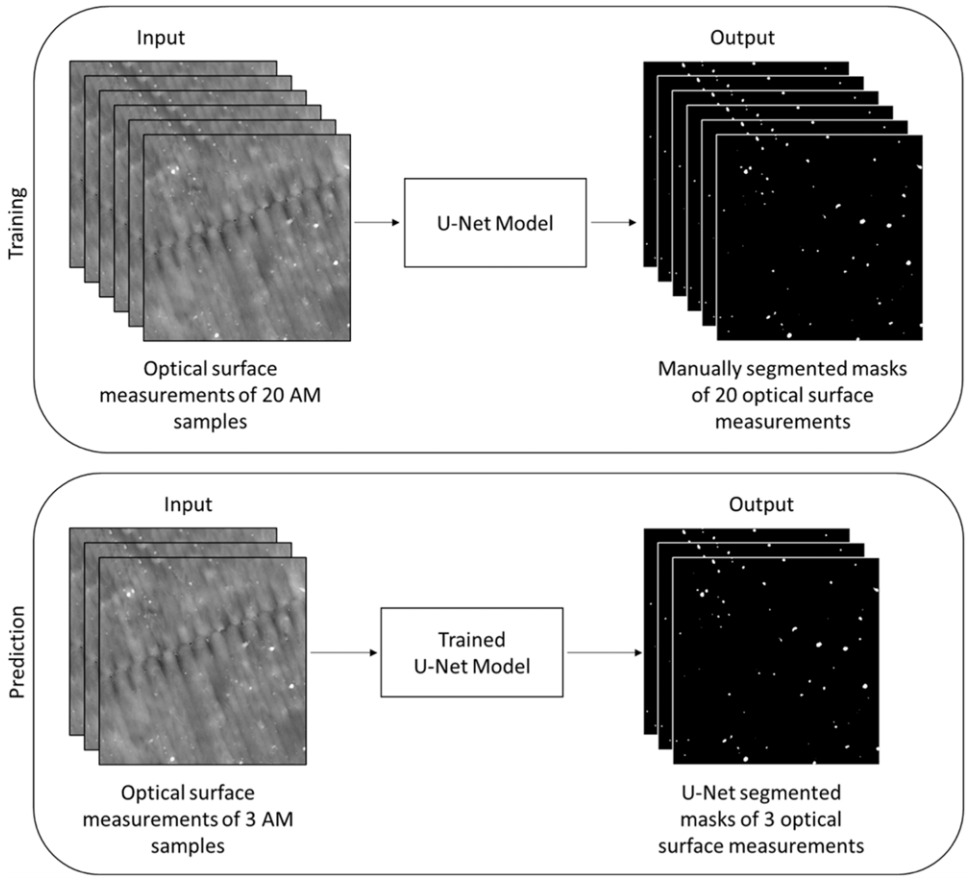

Figure 3. Steps taken to train the U-Net model using optical measurements of 20 AM samples, alongside using the trained model to segment optical measurements of 3 AM samples not used in the training step.

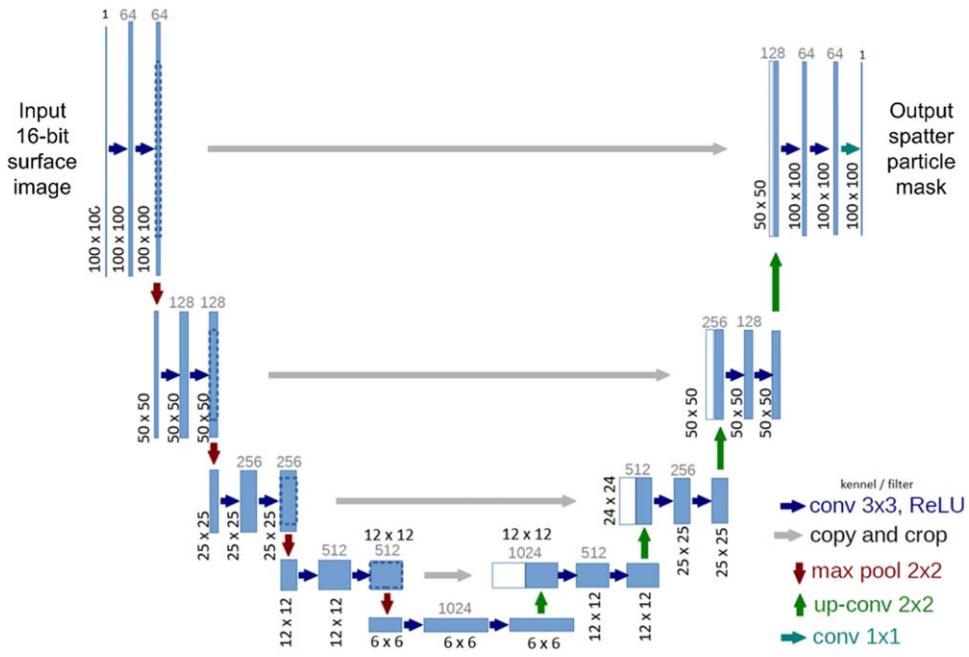

Figure 4. The U-Net architecture adopted in the machine learning based spatter particle segmentation method.

data. Once the model is trained, users simply need to input the surface height data (without applying any high or low pass filters), and the U-Net model will output a spatter particle segmentation mask. The steps taken to train and use the U-Net model for spatter particle segmentation are illustrated in figure 3.

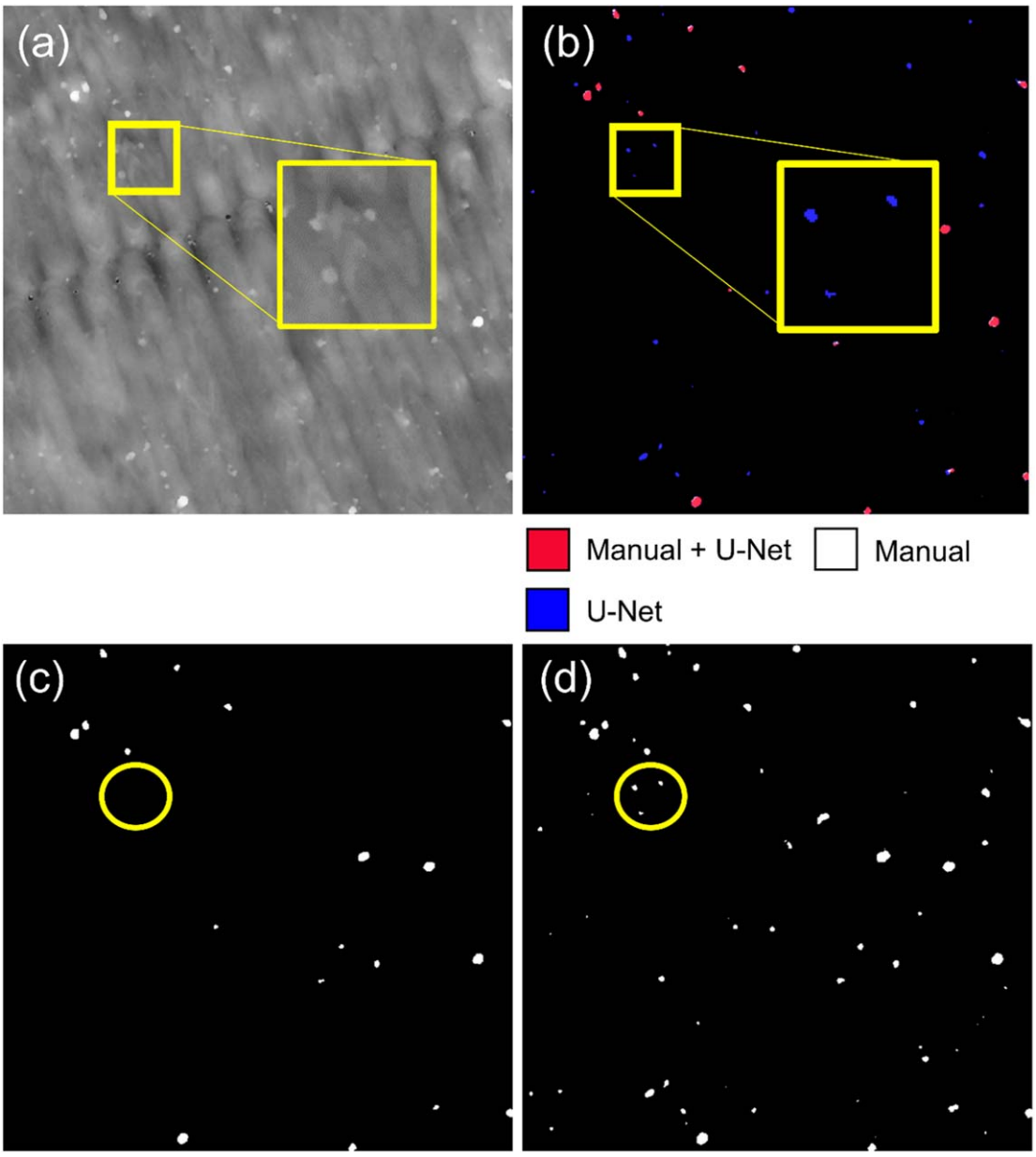

Figure 5. Comparison of segmentation result for sample I11 using the manual segmentation method and the U-Net based segmentation method. (a) surface image of sample I11, (b) combination of the manual threshold and U-Net segmentation results, (c) manual threshold result only, (d) U-Net segmentation result only.

The U-Net architecture adopted for this application is shown in figure 4. The loss function used is the binary cross-entropy loss, and the activation function used is the sigmoid activation function. Both functions are chosen as they are commonly used for binary classification tasks. The U-Net model is trained using 1008 sub-masks, 100 epochs, and a batch size of 20. Training the U-Net model on a laptop running Windows 11 Pro, equipped with a 12th Gen Intel(R) Core(TM) i7-12700H processor clocked at 2.30 GHz and 32 GB RAM, takes approximately 6 h.

2.5. Spatter particle characterisation

The particle segmentation mask generated by the U-Net model enables the evaluation of individual particle characteristics alongside statistics of the particle characteristics for the entire surface. Individual particle characteristics include area, volume, height and diameter, statistics include min, max, mean, standard deviation. These statistics and particle characteristics are evaluated from the particle segmentation mask using a contour finding algorithm in OpenCV [19].

3. Results

A comparison between manual segmentation and the developed U-Net based segmentation of spatter particles for the 3 test samples is given.

Figure 5 shows the segmentation results for the first test sample. The surface data is shown in

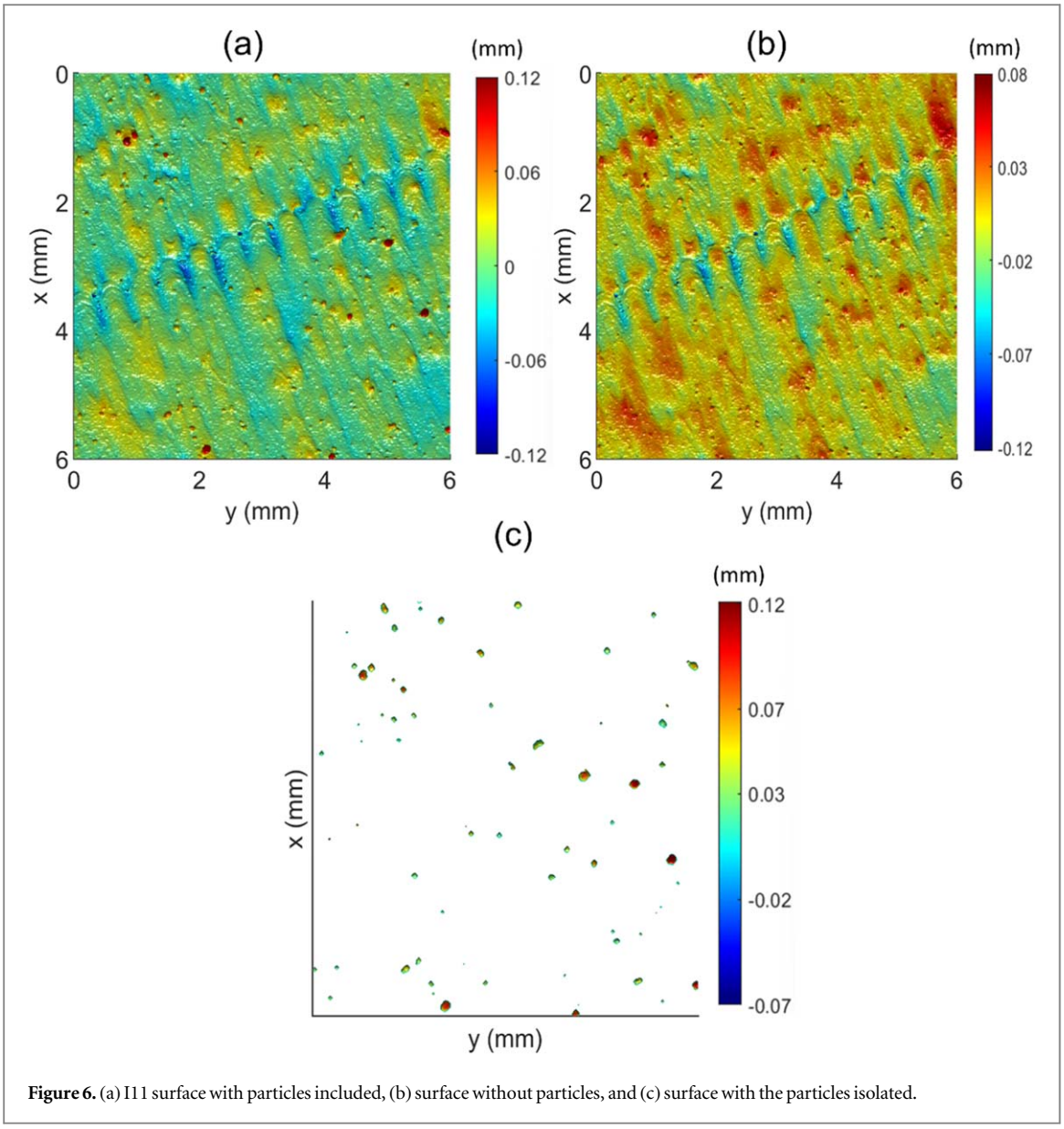

Figure 6. (a) I11 surface with particles included, (b) surface without particles, and (c) surface with the particles isolated.

Table 1. Statistics of detected spatter particles on the I11 surface using the U-Net based segmentation method.

	Area (μm^2)	80% Height (μm)	Volume (μm^3)	Diameter (μm)	Number of particles detected
Min	900.0	0.4	71.8	23.9	
Max	14150.0	52.0	50800.0	94.9	
Mean	3339.5	7.1	2470.0	46.1	61
Std Dev	3531.3	8.9	6260.0	47.4	
Total	190350.0	317.9	168000.0	348.1	

Table 2. Statistics of detected spatter particles on the I11 surface using the manual segmentation method.

	Area (μm^2)	80% Height (μm)	Volume (μm^3)	Diameter (μm)	Number of particles detected
Min	1250.0	1.1	405.0	28.2	
Max	11000.0	52.0	42900.0	83.7	
Mean	5244.0	9.0	4850.0	57.8	18
Std Dev	3303.0	12.5	9620.0	45.9	
Total	94400.0	134.4	87200.0	245.1	

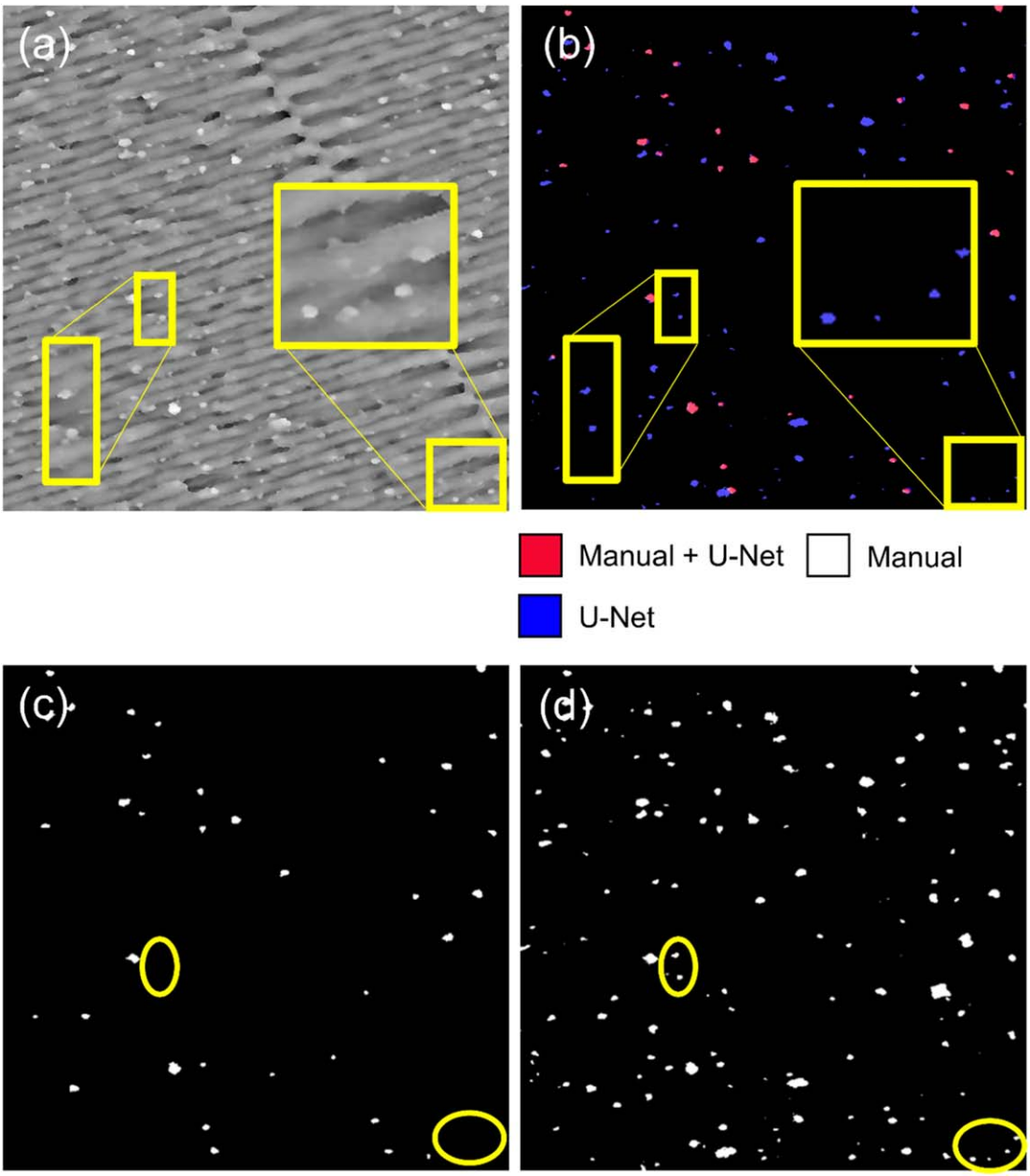

Figure 7. Comparison of segmentation result for sample I9 using the conventional manual segmentation method and the U-Net based segmentation method. (a) surface image of sample I9, (b) combination of the manual threshold and U-Net segmentation results, (c) manual threshold result only, (d) U-Net segmentation result only.

figure 5(a). A comparison of the manual and U-Net segmentation is shown in figure 5(b): red indicates particles detected by both approaches, blue indicates particles detected using the U-Net approach only, white indicates particles detected using the manual approach only. The manual segmentation result is shown in figure 5(c) and exhibits limitations in capturing intricate features, as evidenced by 3 undetected spatter particles highlighted in the figure, these 3 particles are however successfully detected by the U-Net approach shown in figure 5(d).

Figure 6(a) shows the surface of the first test sample as a colourmap. The U-Net particle segmentation mask is used to remove the particles from the surface, the result is shown in figure 6(b). Removing the particles reveals surface details that were previously overshadowed by the particles, for example, the weld-tracks of the surface become easier to visualise. Figure 6(c) shows the segmented spatter particles only, plotted as a heightmap, this is a useful visualisation of particle height, size, and spatial distribution.

Other than facilitating visual inspection of the surface, particle segmentation allows particle statistics to be evaluated. Particle statistics for surface I11 segmented using the U-Net algorithm are given in table 1, whist the characteristics for I11 using manual segmentation are given in table 2, note that an additional 41 spatter particles were detected using the U-Net algorithm. It is possible to evaluate many more particle statistics than those given, but a selection is provided as an example of how

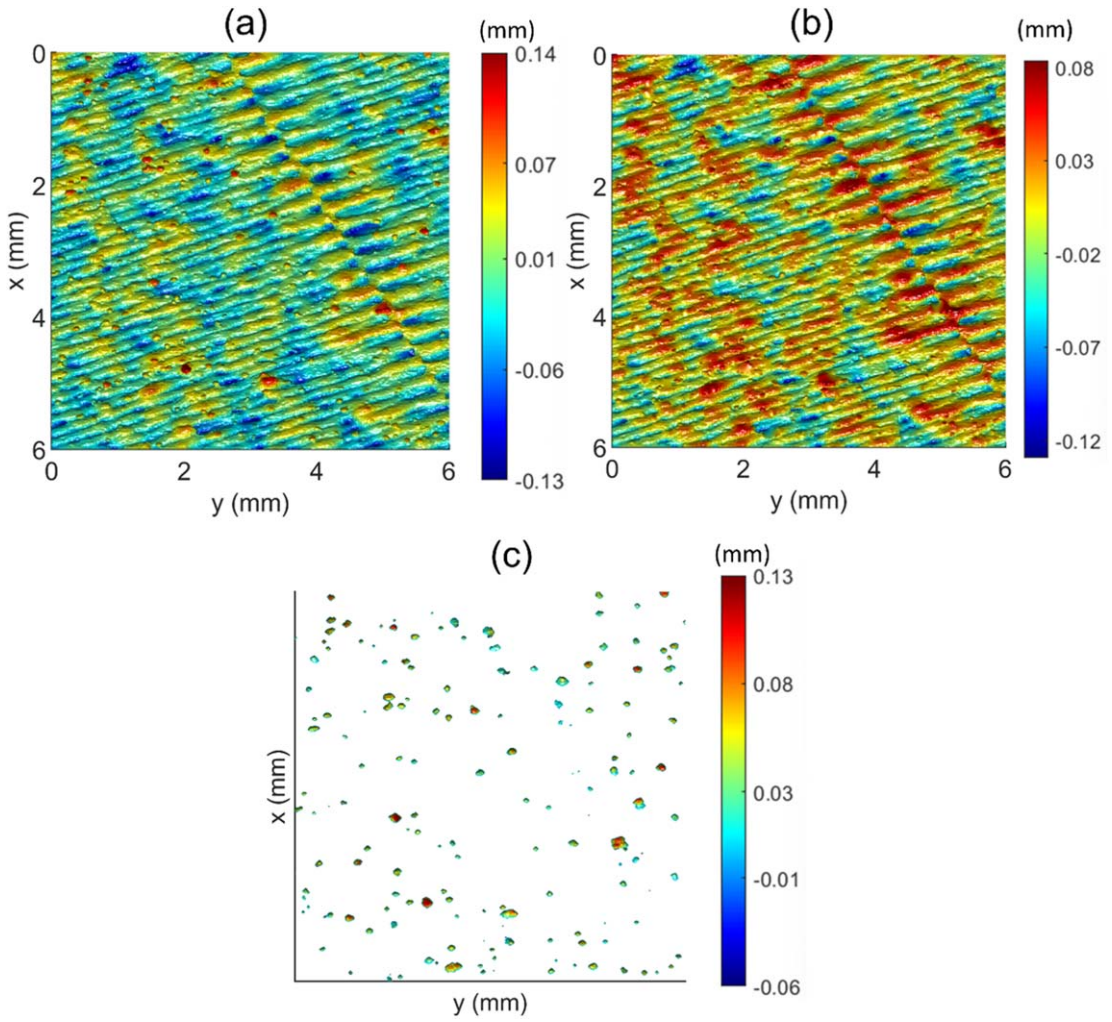

Figure 8. (a) I9 surface with particles included, (b) surface without particles, and (c) surface with the particles isolated.

Table 3. Statistics of detected spatter particles on the I9 surface using the U-Net based segmentation method.

	Area (μm^2)	80% Height (μm)	Volume (μm^3)	Diameter (μm)	Number of particles detected
Min	900.0	0.4	1.5	23.9	
Max	26600.0	70.4	51000.0	130.1	
Mean	3574.0	14.7	7830.0	47.7	148
Std Dev	3975.1	10.9	9242.3	50.3	
Total	514650.0	1988.1	1270000.0	572.4	

Table 4. Statistics of detected spatter particles on the I9 surface using the manual segmentation method.

	Area (μm^2)	80% Height (μm)	Volume (μm^3)	Diameter (μm)	Number of particles detected
Min	1000.0	1.9	242.0	25.2	
Max	13000.0	55.9	41000.0	91.0	
Mean	3998.6	13.6	8310.0	50.5	36
Std Dev	2548.7	10.5	8700.0	40.3	
Total	143950.0	421.5	299000.0	302.7	

the segmentation tool might be used to inform engineering decisions about the quality of the AM surface.

Figure 7(a) shows the surface of the second test sample. As for the first sample, the U-Net segmentation detects particles that are missed by the manual approach, as highlighted by the many blue coloured particles in figure 7(b). A side-by-side comparison of the segmentation results is given in figures 7(c) and (d). Figure 8(a) shows the surface as a height map, alongside the surface with the particles removed 8(b)

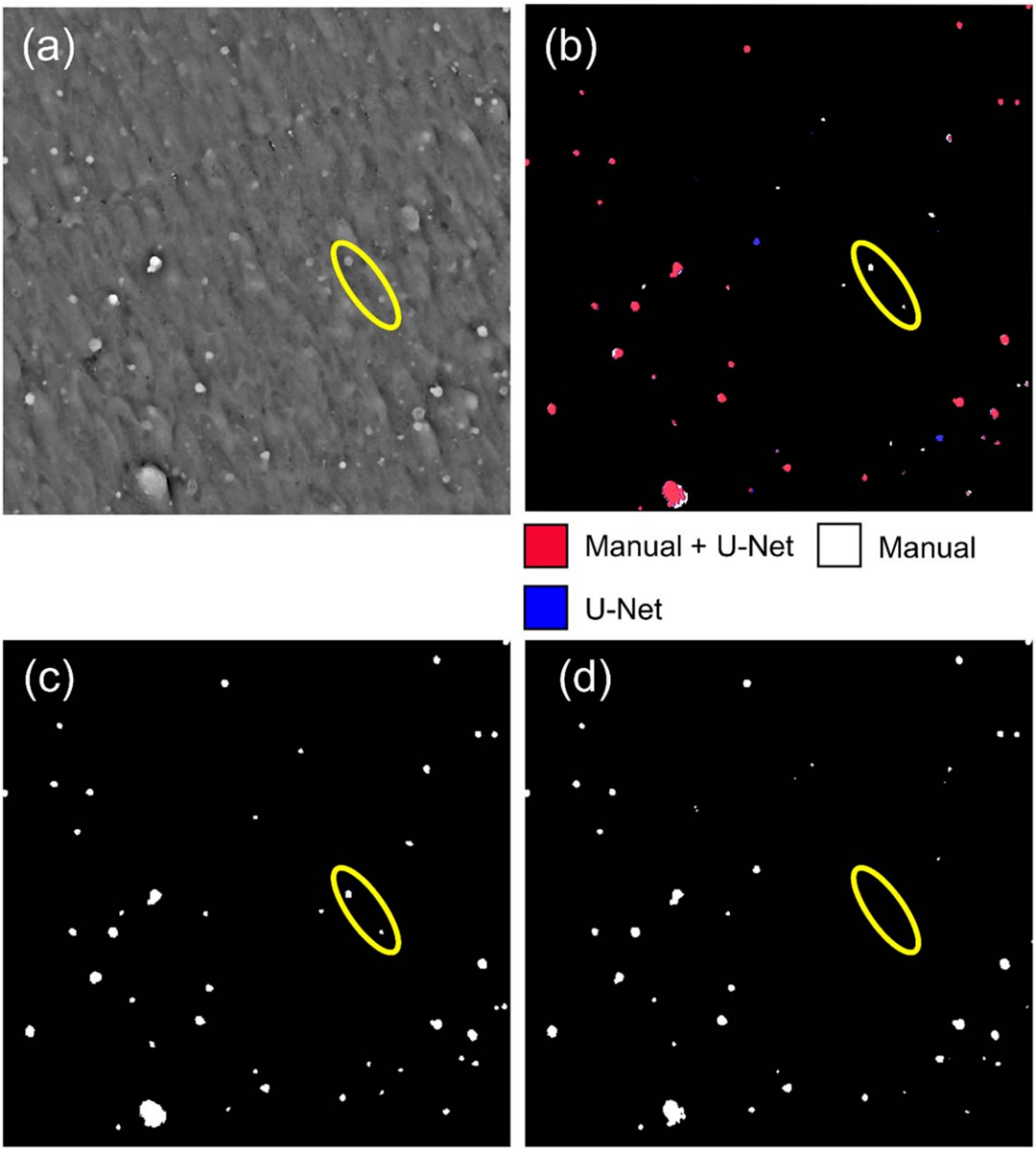

Figure 9. Comparison of segmentation result for sample G1 using a manual segmentation method and a U-Net based segmentation method. (a) surface image of sample G1, (b) combination of the manual threshold and U-Net segmentation results, (c) manual threshold result only, (d) U-Net segmentation result only.

and particles only 8(c). As before, this visualisation reveals greater detail of the weld-tracks when the particles are removed.

Table 3 lists the characteristics of surface I9 segmented using the U-Net algorithm, whilst table 4 lists the characteristics of I9 segmented using manual segmentation, note that an additional 112 spatter particles were detected using the U-Net algorithm. Comparing the values in tables 3 and 4 to tables 1 and 2, it is seen that the surface I9 has more particles than I11, leading to to the total particle area for the I9 surface being much larger.

Figure 9 presents a scenario where the U-Net segmentation has missed some particles despite successfully capturing intricate features in the previous examples. The third surface is shown in figure 9(a), the particles missed by the U-Net segmentation are coloured white in figure 9(b). A side-by-side comparison of the segmentation results is given in figures 9(c) and (d). The lower performance of the U-Net segmentation may be due to the presence of a very large particle in the bottom left of the surface, perhaps this large particle causes smaller particles to be overshadowed and missed by U-Net due to the limited bandwidth of the 16-bit data type used to represent the surface data.

Removing the particles using the mask is not as effective for the third surface as for the previous two, as shown in figures 10(a) and (b). This is again due to the large particle in the bottom left of the surface; even after being removed, its base is still high in comparison to other surface features, thus not as much additional surface detail is revealed when compared the previous two surfaces.

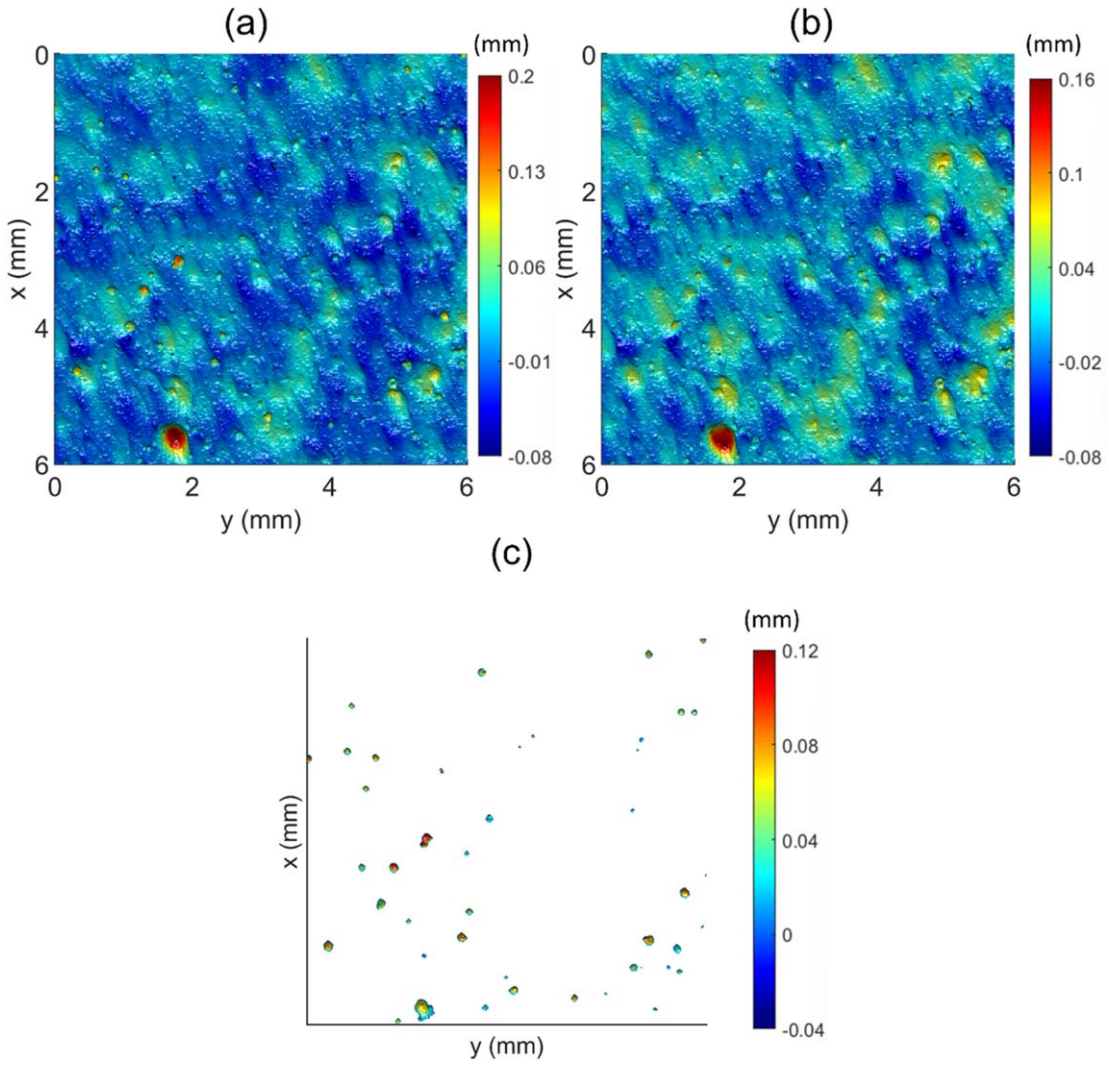

Figure 10. (a) G1 surface with particles included, (b) surface without particles, and (c) surface with the particles isolated.

Table 5. Statistics of detected spatter particles on the G1 surface using the U-Net based segmentation method.

	Area (μm^2)	80% Height (μm)	Volume (μm^3)	Diameter (μm)	Number of particles detected
Min	950.0	0.6	77.4	24.6	
Max	49050.0	40.4	24700.0	176.7	
Mean	5138.1	9.7	4330.0	57.2	43
Std Dev	7834.3	10.3	5997.0	70.6	
Total	215800.0	369.5	195000.0	370.7	

Table 6. Statistics of detected spatter particles on the G1 surface using the manual segmentation method.

	Area (μm^2)	80% Height (μm)	Volume (μm^3)	Diameter (μm)	Number of particles detected
Min	950.0	0.2	1.9	24.6	
Max	67350.0	66.3	34300.0	207.1	
Mean	5776.7	8.6	4450.0	60.6	45
Std Dev	9952.6	11.4	7124.8	79.6	
Total	259950.0	316.9	200000.0	406.8	

The feature statistics for the third surface (G1) are given in tables 5 and 6 for the U-Net segmentation and manual segmentation, respectively. Note that the manual and U-Net segmented particle characteristics are very similar, unlike the first two surfaces, and that the U-Net algorithm detected 2 fewer particles then

the manual approach. The surface has the fewest number of particles when segmented using U-Net, however it does not have the smallest total particle area, this is because the mean particle area of the third surface is larger than the first, indicating that the third surface has fewer, but larger particles than the first surface; this kind of feature based characterisation is expected to be very useful to engineers working on optimising the quality of additively manufactured surfaces by varying process parameters.

4. Discussion

A U-Net based spatter particle segmentation algorithm has been developed for characterising metal additively manufactured surfaces. The results show that for 2 of 3 samples tested, the developed approach can successfully segment spatter particle features that are otherwise missed by a manual, subjective segmentation approach. However, for one of the considered samples, the U-Net approach missed some obvious particles, thus there is room for improvement.

The appeal of the developed approach is that once trained, the segmentation algorithm does not require any variables to be adjusted by subjective human operators. This means that two operators with different levels of experience and skill can process the same data and arrive at the same result, whist for the manual segmentation approach used here, the operator must select a high-pass filter wavelength, a height threshold, and a circularity threshold, a slight change in these parameters will influence the segmentation result.

The disadvantage of the proposed approach is the need for sufficient, good quality training data. Generating good quality training data is a labour-intensive process, and having sufficient training data is sometimes difficult due to limited resources.

It is desirable to determine the accuracy of the developed method for segmenting and characterising spatter particles, however, this would require developing an AM sample with calibrated spatter particles. This is beyond the scope of the present work, but developing AM samples with calibrated surface features is highly desirable as it will allow interlaboratory comparisons of measurement instruments, this will be considered in future work.

In future work, we will continue to train the developed U-Net model and use it with a view to characterise AM surface roughness as a function of print parameters, we expect to then be able to select print parameters that yield the surface characteristics that we desire. For example, minimising the number of spatter particles, and the total particle area, alongside minimising the mean particle height. Future work could also include developing segmentation algorithms for different surface features, such as cracks, or surface breaking pores.

5. Conclusions

It can be concluded that a U-Net based spatter particle segmentation algorithm can detect AM surface features that are not be detectable using a manual segmentation approach. The results showed that the implemented U-Net algorithm detected 43 and 112 additional spatter particles for samples 1 and 2 respectively, however, for sample 3 the U-Net algorithm missed 2 spatter particles. Based on these results we recommend further training of the U-Net approach is required before it can fully supersede manual segmentation.

This work demonstrates that machine learning based segmentation algorithms are well-suited for the segmentation of additively manufactured surfaces, since these surfaces have well-defined and reproduceable surface features, such as spatter particles. The disadvantage of a machine learning approach is the need for a sufficient number of high-quality training data sets; generating such training data is a manual time-consuming process.

This work demonstrates that the U-Net segmentation algorithm can be used to minimise user influence in feature-based surface characterisation; users simply need to input the surface data and the algorithm will segment the surface automatically. Subsequent characterisation of the segmentation result can also be automated, thus removing the human operator from the entire surface characterisation process. Such an approach could be adopted to automate a quality control process in a production environment, or to automate process optimisation in a research and development environment.

Acknowledgments

This research is supported by the Agency for Science, Technology and Research (A*STAR), Singapore, under the Central Research Fund.

Data availability statement

We will share the data when requested to do so. The data cannot be made publicly available upon publication due to legal restrictions preventing unrestricted public distribution. The data that support the findings of this study are available upon reasonable request from the authors.

Appendix

ID	Infill - Laser power/W	Infill - Scan speed/ mm/s	Infill - Hatch distance/ mm	Contour - Laser power/W	Contour - Scan speed/ mm/s
A10	370	1400	0.273	162	1344
B03	162	800	0.063	90	1232
B12	234	1100	0.063	234	1008
C10	370	1500	0.084	162	336
D05	162	800	0.105	162	672
G01	306	1100	0.147	234	672
G04	306	500	0.189	162	336
H01	90	700	0.168	234	224
H05	90	1100	0.147	306	1008
I01	162	800	0.273	90	560
I04	162	600	0.189	162	336
I09	370	1300	0.189	306	336
I11	90	1100	0.273	162	560
J09	162	1500	0.168	234	1008
J13	234	500	0.21	162	896
K09	90	900	0.21	370	672
L04	306	600	0.126	234	784
L05	162	1200	0.273	370	672
L10	234	1400	0.147	370	672
L12	162	600	0.273	234	224
L13	306	700	0.063	370	448
M04	370	800	0.105	306	784
M12	234	1200	0.063	162	448

ORCID iDs

Hwee Ping Ng https://orcid.org/0009-0000-5833-5012
Ronnie Ssebaggala https://orcid.org/0009-0000-3946-9621
Joseph John Lifton https://orcid.org/0000-0002-8716-1055

References

[1] Lou S, Pagani L, Zeng W, Jiang X and Scott P J 2020 Watershed segmentation of topographical features on freeform surfaces and its application to additively manufactured surfaces *Precis. Eng.* **63** 177–86
[2] Senin N, Thompson A and Leach R 2018 Feature-based characterisation of signature topography in laser powder bed fusion of metals *Meas. Sci. Technol.* **29** 045009
[3] Newton L, Senin N, Smith B, Chatzivagiannis E and Leach R 2019 Comparison and validation of surface topography segmentation methods for feature-based characterisation of metal powder bed fusion surfaces *Surf. Topography: Metrol. Prop.* **7** 045020
[4] MacAulay G, Senin N, Giusca C and Leach R 2014 Comparison of segmentation techniques to determine the geometric parameters of structured surface *Surf. Topography: Metrol. Prop.* **2** 044004
[5] Senin N, Blunt L, Leach R and Pini S 2013 Morphologic segmentation algorithms for extracting individual surface features from areal surface topography maps *Surf. Topography: Metrol. Prop.* **1** 015005
[6] Ozel T, Altay A, Kaftanoglu B, Leach R, Senin N and Donmez A 2020 Focus variation measurement and prediction of surface texture parameters using machine learning in laser powder bed fusion *J. Manuf. Sci. Eng.* **142** 011008
[7] Barik S, Bhandari R and Mondal M K 2023 Optimization of wire arc additive manufacturing process parameters for low-carbon steel and properties prediction by support vector regression model *Steel Res. Int.* **95** 2300369
[8] Tan Z, Fang Q, Li H, Liu S, Zhu W and Yang D 2020 Neural network based image segmentation for spatter extraction during laser-based powder bed fusion processing *Opt. Laser Technol.* **130** 106347
[9] Li J, Shao S and Hong J 2020 Machine learning shadowgraph for particle size and shape characterization *Meas. Sci. Technol.* **32** 015406
[10] Gotkowski K, Gupta S, Godinho J, Tochtrop C, Maier-Hein K and Isensee F 2024 ParticleSeg3D: Scalable, out-of-the-box segmentation of individual particles from mineral samples acquired with micro CT *Powder Technol.* **434** 119286
[11] Luo S, Ma X, Xu J, Li M and Cao L 2021 Deep learning based monitoring of spatter behavior by the acoustic signal in selective laser melting *Sensors* **21** 7179
[12] Mohammed A, Almutahhar M, Sattar K, Alhajeri A, Nazir A and Ali U 2023 Deep learning based porosity prediction for addictively manufactured laser power-bed fusion parts *J. Mater. Res. Technol.* **27** 7330–5
[13] Li Z *et al* 2022 A review of spatter in laser power bed fusion addictive manufacturing: *In Situ* detection, generation, effects, and countermeasures *Micromachines* **13** 1366
[14] Ronneberger O, Fischer P and Brox T 2015 U-net: convolutional networks for biomedical image segmentation *Proceedings of Medical Image Computing and Computer-Assisted Intervention* **9351** 234–41
[15] Deshpande S, Venugopal V, Kumar M and Anand S 2024 Deep learning-based image segmentation for defect detection in addictive manufacturing: an overview *Int. J. Adv. Manuf. Technol.* **134** 2081–105
[16] Dursun G, Ibekwe S, Li G, Mensah P, Joshi G and Jerro D 2020 Influence of laser processing parameters on the surface characteristics of 316L stainless steel manufactured by selective laser melting *Mater. Today Proc.* **26** 387–93
[17] Dai S, Liao H, Zhu H and Zeng X 2022 The mechanism of process parameters influencing the AlSi10Mg side surface quality fabricated via laser powder bed fusion *Rapid Prototyping Journal* **28** 514–24
[18] Zhang T and Yuan L 2024 Melt Pool characteristics on surface roughness and printability of 316L stainless steel in laser powder bed fusion *Rapid Prototyping Journal* (https://doi.org/10.1108/RPJ-02-2024-0078)
[19] OpenCV Open Source Computer Vision https://docs.opencv.org/4.x/d6/d00/tutorial_py_root.html accessed online